Clays and Clay Minerals, Vol. 29, No. 5, 365–377, 1981.

ZEOLITE MINERAL REACTIONS IN A TUFF IN THE LANEY MEMBER OF THE GREEN RIVER FORMATION, WYOMING

NANCY G. RATTERMAN AND RONALD C. SURDAM
Department of Geology, University of Wyoming, Laramie, Wyoming 82071

Abstract—Two diagenetic stages of zeolitic alteration were recognized in a study of a thin bed of rhyolitic ash that was deposited in Eocene Lake Gosiute (Laney Member of the Green River Formation). The ash bed can be traced for 30 km along strike and represents a single volcanic event. The bed was not buried deeply (<100°C), and originally it was compositionally homogeneous. Initially, the bed altered to clinoptilolite, heulandite, an intermediate phase between these two zeolites, and mordenite. These early reactions involved the hydration and solution of glass by saline, alkaline solutions and the subsequent precipitation of zeolites. The variation in zeolite mineralogy is due to differences in interstitial fluid chemistry that resulted from either fluctuations in lake-water chemistry or the proximity of spring discharge. These reactions, exclusive of the addition of H_2O, involved only minor amounts of mass transfer over very small distances. Later, after burial, the early-formed zeolites reacted with upward moving sodium carbonate brines that were produced by dewatering of underlying evaporite deposits. The sodium carbonate brines, in equilibrium with trona and nahcolite, elevated the activity of Na^+ and produced analcime. These later dehydration reactions involved significant mass transfer.

Key Words—Analcime, Clinoptilolite, Diagenesis, Green River Formation, Heulandite, Volcanic ash, Zeolites.

INTRODUCTION

This investigation delineates the diagenetic history of a single, thin tuff bed that was deposited in Eocene Lake Gosiute, a saline, alkaline lake. This tuff bed is of special interest because it can be traced along strike for about 30 km and can be sampled continuously. The bed was chosen for study because it has undergone only shallow burial, it is well exposed, and it contains a variety of diagenetic minerals. It also illustrates the variable mineral content of such zeolitically altered tuffs both vertically and horizontally over short distances.

General geology

The Green River Formation is a sequence of lacustrine strata covering an area of 43,500 km² in southwestern Wyoming and adjoining parts of Utah and Colorado (Bradley, 1964). Sediments of early to middle Eocene age were deposited in Lake Gosiute over a period of 8 million years. Low topographic gradients and climatic fluctuations caused frequent transgressions and regressions of the shallow lake over the surrounding broad mudflats in a basin which was hydrographically closed until the lake's latest stages (Surdam and Stanley, 1979). Progressive tectonic downwarping of the basin during Green River deposition resulted in a thick accumulation of sediments (Bradley and Eugster, 1969).

In Wyoming, the Green River Formation is divided in ascending order into the Tipton Shale, the Wilkins Peak, and the Laney Members (Bradley, 1964). The Wilkins Peak Member represents a general minimum stand of the lake, and the Tipton Shale and Laney Members represent maximum stands. The area of interest in this study is the western Washakie Basin (Figure 1).

Stratigraphy of the Laney Member

The Laney Member of the Green River Formation represents the time when Lake Gosiute evolved from a saline, alkaline lake to a fresh-water lake having a southward outlet into the Piceance Creek Basin (Surdam and Stanley, 1979). The dominant lithology of the Laney Member is repetitive sequences of fine-grained lacustrine carbonate rocks that are related to transgressions and regressions of the lake and are diluted by siliciclastic detritus near the basin margins (Buchheim, 1978).

Roehler (1973) divided the Laney Member in the Washakie Basin into three units: (1) the lower LaClede Bed, a basal, kerogen-rich carbonate unit; (2) the overlying Sand Butte Bed that contains tuffaceous sandstone and siltstones; (3) and the upper Hartt Cabin Bed, a sequence of mudstone alternating with sandstone, limestone, and shale (Figure 2).

This investigation is a detailed study of a 2-m thick stratigraphic interval in the LaClede Bed deposited when the lake basin was still hydrographically closed. This stratigraphic interval is about 5–6 m above the Buff Marker Bed of Surdam and Stanley (1979) (Figure 3). The interval consists of calcium-rich, laminated, kerogenous carbonates which are a part of a transgressive depositional sequence commonly overlying a stromatolitic, oolitic, or ostracodal basal unit (Surdam and Stanley, 1979). Several 0.2- to 0.8-cm thick tuff beds

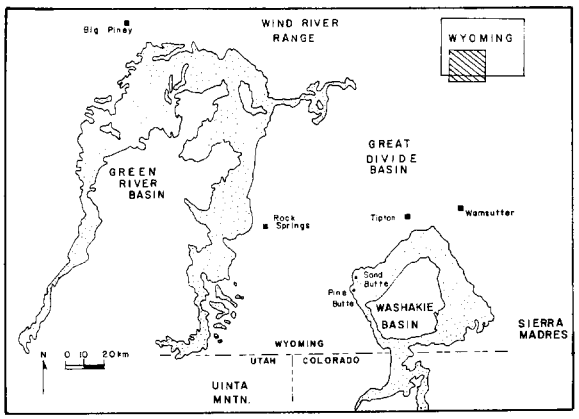

Figure 1. Index map of the Laney Member of the Green River Formation in southwestern Wyoming. The area of investigation is the western half of the Washakie Basin.

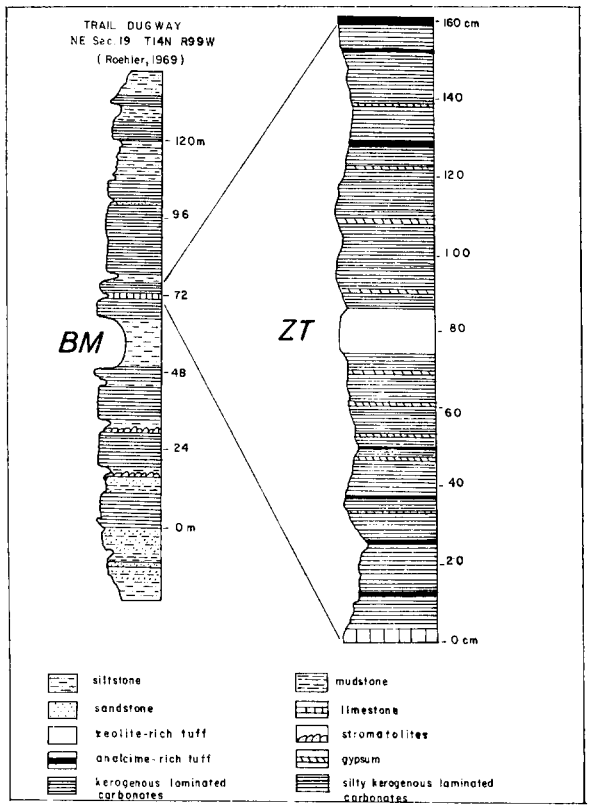

Figure 2. Generalized stratigraphic column of the LaClede Bed (lower portion of the Laney Member of the Green River Formation). Figure also shows the detailed section of the stratigraphic interval sampled in this study. The Buff Marker Bed (BM) is at approximately 48–65 m and the zeolitized tuff (ZT) is at 80 m.

altered to analcime form continous planes of correlation within the interval. The unit studied in detail is a 12–16-cm thick tuff bed (ZT) that is traceable for 30 km along the outcrop. Contacts between the tuff and the carbonates above and below are sharp, and no evidence of mudcracks or aerial exposure immediately before, after, or during deposition was found.

METHODS OF STUDY

Samples were collected along the western boundary of the Washakie Basin on the Kinney Rim, where the tuff bed forms a resistant ledge (Figure 3). Samples of the tuff were taken at regular intervals or wherever an obvious change in lithology was observed. At selected locations, short stratigraphic sections were measured, and strata were sampled in detail above and below the tuff (Figure 4). More than 100 samples of the tuff were collected, the locations of which are shown in Figure 4, and seven sections were measured. The mineral content of all samples was determined by X-ray powder diffraction (XRD) techniques using a GE XRD-5 instrument and Ni-filtered CuKα radiation (Table 1). Near-monominerallic fractions for chemical analysis were prepared by gravity separation using diluted heavy liquids. XRD patterns and optical examination in immersion oil generally showed less than 5% impurities in the separates; however, corrections were not made for these impurities. Chemical analyses of the purified separates were made using atomic absorption spectroscopy and ion-selective electrodes (Tables 2 and 3), and recalculated on the basis of 72 oxygens per unit cell for heulandite-group minerals and 96 oxygens per unit cell for analcime. Scanning electron microscopy (SEM) was carried out with a JEOLCO instrument.

MINERALOGY

Description of the tuff

The tuff bed of this study was originally a crystal, vitric ash composed of volcanic dust and glass shards

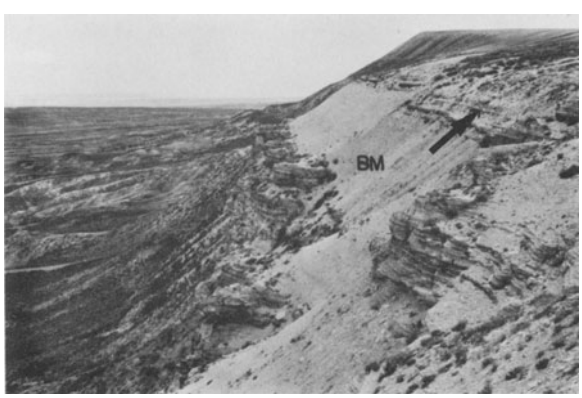

Figure 3. The LaClede Bed at Sand Butte (T16N, R100W) showing Buff Marker Bed (BM) and the tuff (ZT) of this study (arrow).

https://doi.org/10.1346/CCMN.1981.0290506 Published online by Cambridge University Press

Table 1. Mineralogy of tuff samples determined by X-ray powder diffraction.

Sample number	Location in tuff bed	Anal	Heul	Clin	Int-H	Mord	Qtz	Feld	Biot	Gyp	Others
16-T	M	T	A	—	—	T	P	P	—	T	Calc
13-T	M	—	A	—	—	T	P	—	—	T	—
14-T	M	—	A	—	—	T	P	P	T	—	tr glass, tr clay
14-T1	L	—	A	—	—	P	P	T	T	—	—
14-T2	U	—	A	—	—	—	P	T	T	P	tr glass
14-T3	U	—	A	—	—	T	P	—	—	T	—
15-T1	U	—	A	—	—	T	P	—	—	—	tr glass
15-T2	U	—	A	—	—	T	P	T	T	—	tr glass
15-T3	L	—	A	—	—	P	T	—	T	—	tr glass
15-TSB	L	—	A	—	—	P	A	P	T	P	—
S4-T1	L	—	—	—	A	P	P	P/A	T	—	T
S4-TSA	U	—	A	—	—	P	T	—	—	—	—
S5-T1	M	T	—	A	—	T	—	T	—	P	—
S5-T2	L	T	—	—	A	P	T	P	T	T	—
4-T	M	—	—	A	—	T	T	P	—	—	tr Calc
4-T2	U	—	—	A	—	T	T	—	T	T	tr Calc
4-5-T	U	T	A	—	—	T	T	—	T	—	—
4-5-rp	M	P	A	—	—	—	T	T	—	T	—
4-5-SB	L	T	A	—	—	T	P	—	T	T	—
5-T1	U	T	—	A	—	T	T	T	T	T	—
5-T2	M	T	—	A	—	T	T	—	T	P	—
5-T3	L	—	—	A	—	—	T	P	T	P	—
5-T4	L	—	—	—	A	P	A	—	T	T	—
3-T1	U	—	—	—	A	P	P	P	T	T	—
3-T2	M	—	—	—	A	T	T	T	T	T	—
3-T3	U	T	—	—	A	P	T	T	—	T	—
3-T4	U	T	—	—	A	P	T	—	T	—	—
S2-T	L	—	—	A	—	P	T	P	T	—	—
S2-T2	U	T	—	A	—	P	T	—	T	—	—
6-P*	M	T	—	A	—	P	T	—	T	T	—
7-T	U	—	—	A	—	P	T	—	—	T	—
7-T2	L	—	—	A	—	T	—	—	—	—	—
7-T3	M	—	—	A	—	T	—	—	T	—	—
7-SB1	L	—	—	A	—	P	A	—	T	—	—
8-T1	L	T	A	—	—	T	P	P	T	—	—
8-T2	L	—	A	—	—	T	T	—	—	—	—
8-T3	L	—	A	—	—	P	T	—	—	T	—
S3-T1	M	T	—	—	A	T	T	—	—	—	—
25-T1	U	—	—	A	—	T	T	—	—	—	—
25-T2	M	T	—	A	—	P	T	—	—	—	—
25-T3	M	T	—	A	—	P	T	—	—	—	—
27-T	L	P	—	—	A	—	T	—	—	T	—
27-T1	U	T	—	—	A	T	T	—	T	T	—
9-T	U	P	A	—	—	—	T	—	T	T	—
9-T1	M	P	A	—	—	—	T	—	—	P	—
9-TB	L	P	A	—	—	P	A	—	—	—	—
26-T	M	A	—	A	—	—	T	T	—	T	—
SBT	L	P	P	—	—	—	A	—	—	—	—
SBA	M	P	P	—	—	T	T	T	T	—	—
S1-T	M	T	A	—	—	—	T	T	T	—	—
S1-TA	N	A	P	—	—	—	T	—	T	—	—
S1-T2	N	A	T	—	—	—	P	P	T	A	—
S1-T3	U	A	T	—	—	—	P	T	—	—	—
S1-T4	U	A	—	—	P	T	P	T	T	T	—
S1-T6	U	P	A	—	—	—	T	T	—	T	—
S1-T7	U	A	—	—	P	—	T	T	—	—	tr Calc
S1-T9A	N	A	A	—	—	—	P	P	T	T	—
S1-T9	M	A	—	—	A	—	P	T	T	T	—
10-T1	M	T	—	A	—	—	T	—	—	T	—
10-T2	N	A	—	—	—	—	P	T	—	T	—
S1-T10A	N	A	T	—	—	—	T	T	—	—	—
S1-T10	M	T	A	—	—	—	T	T	T	—	—
22-TA	N	A	—	—	—	—	T	T	—	T	—

https://doi.org/10.1346/CCMN.1981.0290506 Published online by Cambridge University Press

Table 1. Continued.

Sample number	Location in tuff bed	Anal	Heul	Clin	Int-H	Mord	Qtz	Feld	Biot	Gyp	Others
22-T	M	P	—	A	—	—	T	T	—	T	—
24-T1	U	T	—	—	A	—	T	T	T	—	—
24-T2	M	P	—	—	A	T	T	—	—	T	—
11-T	M	T	A	—	—	—	T	—	—	—	—
10-T1	U	T	A	—	—	T	T	T	T	T	—
19-T2	M	T	A	—	—	T	T	T	T	—	—
18-T1	N	A	T	—	—	—	T	P	—	T	—
18-T2	U	P	A	—	—	—	T	T	T	T	—
S6-T2	N	A	—	—	—	—	A	T	—	P	—
S6-T3	N	A	—	—	—	—	P	T	—	P	—
17-T	U	P	A	—	—	—	T	T	T	P	—
17-T2	N	A	—	—	—	—	A	P	T	T	—
S7-T	M	T	A	—	—	T	T	P	T	P	—
S7-T2	U	T	A	—	—	T	P	P	—	—	—
45-T	L	T	—	—	A	T	P	—	—	—	Calc
46-T	U	—	A	—	—	T	T	—	—	—	—
47-T	L	T	A	—	—	T	T	—	—	—	—
48-T	L	T	—	—	A	—	A	—	—	—	tr Calc
49-T1	L	T	A	—	—	T	T	—	—	T	—
49-T2	L	T	A	—	—	T	T	—	T	P	—
43-T1	M	—	—	A	—	—	T	?	—	—	—
43-T2	T	—	A	—	—	T	P	T	—	—	—
44-TA	N	A	—	—	—	—	T	P	—	P	—
44-T*	M	—	—	A	—	—	T	T	T	T	—
TDA	N	A	—	—	—	—	A	P	—	—	—

Symbols: U = upper part of tuff, M = middle part of tuff, L = lower part of tuff, N = nodule, A = abundant, P = present, T, tr = trace, — = not detected, Anal = analcime, Heul = heulandite, Clin = clinoptilolite, Int-H = intermediate phase between heulandite and clinoptilolite, Mord = mordenite, Qtz = quartz, Feld = feldspar, Biot = biotite, Gyp = gypsum, Calc = calcite.

and 10–20% crystal and lithic fragments. The tuff generally is white or light orange to buff where it is zeolite rich. It is commonly streaked or speckled with a dark rusty orange stain of iron oxide from weathering of biotite and pyrite. The tuff is well indurated and weathers into angular blocks having conchoidal fracture.

The tuff generally is fine grained and graded. Pyroclastic crystals are most abundant and coarsest, up to 0.8 mm in diameter, at the base of the tuff. Where the tuff has altered to an analcime, it is light to dark gray and coarsely crystalline. The analcime crystals are medium to coarse sand-size and either make up the entire thickness of the bed or occur in nodules that have abrupt contacts with the very fine-grained, zeolite-rich tuff (Figure 5). The nodules appear to have grown from the base of the tuff upward, and the analcime crystals generally are smaller upward. Contacts with the carbonates above and below the tuff are sharp both in outcrop and in thin section (Figure 5).

Petrography of the tuff

In thin sections the tuff exhibits a porphyritic texture of unaltered primary pyroclastic crystals, that vary in size from <0.1 mm to as much as 0.8 mm in diameter. The crystals are surrounded by a matrix of authigenic, micrometer-size needles and laths of alkalic zeolites. The pyroclastic crystals are chiefly sanidine and quartz, with minor amounts of finer grained biotite, muscovite, hornblende, and plagioclase. Plagioclase grains are rare, commonly elongate, finely twinned, and too small to be identified optically. Biotite occurs as flakes, and locally it is concentrated at the base of the tuff.

Needles and laths of clinoptilolite, heulandite, and mordenite in the matrix are <0.01 mm in length and are commonly indistinguishable except by SEM. Remnant outlines of glass shards are in most thin sections, except where the tuff is altered to analcime.

The analcime-rich rocks are composed of chains of coarse, interlocked, trapezohedral analcime crystals up to 3.0 mm in maximum dimension (Figure 6). Analcime crystals are mottled brown because of many very fine inclusions. The crystals are generally isotropic, but some are slightly birefringent near the edges. There is no remnant vitroclastic texture in these rocks (Figure 6).

Original composition and depositional environment

Volcanic glass was found in samples taken at one location, about 30 m north of the southeast corner of section 9, T16N, R100W (Figure 4). A rhyolitic composition

https://doi.org/10.1346/CCMN.1981.0290506 Published online by Cambridge University Press

Table 2. Chemical composition and unit-cell contents of heulandite-group minerals from a tuff bed in the Laney Member of the Green River Formation, Wyoming.

	Clinoptilolites				Heulandites					Int. H-C[1]	Mordenite[2]
	4-T2	5-T3	25-T1	7-T	S7-T2	8T2	11-T	14-T3	15-T2	24-T1	
SiO_2	60.0	63.0	66.8	62.5	65.9	63.7	60.9	61.0	62.2	58.5	66.31
Al_2O_3	10.0	10.6	11.1	10.8	10.7	10.9	10.8	10.9	10.6	10.28	11.52
Fe_2O_3	1.75	2.79	0.50	1.96	0.42	0.60	1.79	2.19	1.22	1.11	0.67
Na_2O	4.85	3.19	3.13	4.75	1.10	1.65	1.51	1.07	1.68	2.05	3.09
K_2O	0.90	1.65	0.87	1.24	0.99	0.87	1.04	1.16	1.47	1.26	0.96
CaO	2.06	2.00	1.61	1.81	3.60	3.48	3.87	3.59	3.05	2.24	2.58
MgO	1.03	0.66	1.46	0.73	1.17	0.95	0.99	1.62	0.88	1.65	0.54
TiO_2	0.0	0.00	0.1	0.0	0.0	0.0	0.1	0.0	0.0	0.1	0.12
MnO	0.0	0.01	0.01	0.01	0.01	0.02	0.02	0.00	0.02	0.00	0.00
Total	80.59	83.85	85.60	83.79	83.88	82.23	81.10	81.43	81.09	91.5	85.79
Unit-cell content based on 72 oxygens											
Si	29.56	29.24	29.94	29.34	30.10	29.78	29.24	29.10		29.83	19.78
Al	5.80	5.79	5.89	5.97	5.75	6.01	6.11	6.12		5.77	4.05
Fe^{3+}	0.64	0.97	0.17	0.69	0.14	0.21	0.65	0.78		0.40	0.15
Na	3.36	2.88	2.46	4.26	0.86	1.36	1.28	0.90		1.60	1.79
K	0.40	0.98	0.44	0.74	0.52	0.48	0.58	0.64		0.65	0.37
Ca	0.78	1.12	0.70	0.90	1.56	1.58	1.80	1.66		0.97	0.82
Mg	0.54	0.46	0.88	—	0.68	0.60	0.64	1.04		0.99	0.24
O	72.00	72.00	72.00	72.00	72.00	72.00	72.00	72.00		72.00	72.00
$Si + Al + Fe^{3+}$	36.00	36.00	36.00	36.00	36.00	36.00	36.00	36.00		36.00	36.00
$Si:(Al + Fe^{3+})$	4.58	4.32	4.94	4.41	5.10	4.79	4.33	4.21		4.52	4.71
Si:Al	5.10	5.05	5.09	4.92	5.23	4.96	4.79	4.75		4.83	4.88

[1] Intermediate heulandite-clinoptilolite.

[2] Mordenite from Barstow Formation, California (Sheppard and Gude, 1969, p. 15).

Major cations determined by atomic absorption spectroscopy; Si by colorimetric procedure using a UV-VIS spectrophotometer.

Table 3. Chemical composition and unit-cell contents of analcimes from a tuff bed in the Laney Member of the Green River Formation, Wyoming.

	S1-T10A	S1-T4	18-T1	44-TA	10-T2	S6-T3	22-TA	TDA
SiO_2	59.4	59.6	59.2	54.3	55.4	56.5	58.8	65.6
Al_2O_3	16.5	16.5	16.7	15.9	15.6	16.6	16.3	13.6
Fe_2O_3	1.89	0.36	1.13	4.85	1.54	2.34	1.60	2.22
Na_2O	11.96	10.29	11.49	9.35	11.60	10.77	10.20	8.13
K_2O	0.53	0.68	0.69	0.71	0.70	0.66	0.57	0.62
CaO	0.31	0.77	0.70	0.71	2.46	2.39	0.36	0.28
MgO	0.05	0.08	0.05	0.26	0.12	0.09	0.06	0.05
TiO_2	0.0	0.0	0.0	0.0	0.0	0.0	0.1	0.1
MnO	0.00	0.00	0.01	0.04	0.00	0.02	0.01	0.01
Total	90.47	88.24	89.95	86.11	87.47	88.36	88.0	90.6
Unit-cell content based on 96 oxygens								
Si	35.56	36.07	35.65				35.64	
Al	11.63	11.76	11.84				11.63	
Fe^{3+}	0.81	0.16	0.51				0.73	
Na	11.69	10.48	11.10				11.40	
K	0.34	0.45	0.44				0.42	
Ca	0.33	0.86	0.74				0.44	
Mg	0.08	0.13	0.07				0.10	
O	96.00	96.00	96.00				96.00	
$Si + Al + Fe^{3+}$	48.00	48.00	48.00				48.00	
$Si: (Al + Fe^{3+})$	2.86	3.02	2.89				2.88	
Si:Al	3.06	3.07	3.01				2.90	

Major cations determined by atomic absorption spectroscopy; Si by colorimetric procedure using a UV-VIS spectrophotometer.

https://doi.org/10.1346/CCMN.1981.0290506 Published online by Cambridge University Press

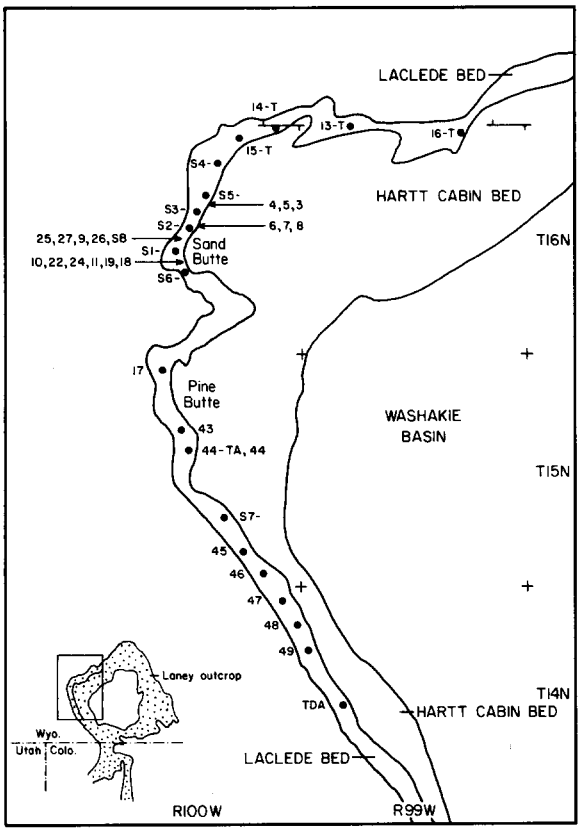

Figure 4. Sample locations along the Kinney Rim.

Figure 5. Coarse analcime nodule that replaced the surrounding alkalic zeolites in the tuff (ZT). Note the fractures in the underlying oil shale. These fractures served as pathways for concentrated brines emanating from the underlying evaporite facies (Buff Marker Bed of Figure 3).

for the glass was confirmed by chemical analysis. Observations pertinent to interpreting the depositional environment of the ash are: (1) the ash has sharp contacts with the laminated carbonates above and below; (2) the ash consistently becomes finer grained upward, with concentrations of denser pyroclastic grains at the base; (3) the pyroclastic grains are angular; (4) the ash has lateral uniformity in thickness, grain-size distribution, and composition; and (5) no field evidence exists that suggests reworking or sorting of the ash constituents. Thus, the tuff appears to have been deposited as vitric ash by airfall directly in the lake where the ash settled through the water column and underwent minor sedimentary reworking or lateral transport.

The source of pyroclastic debris in the Green River Formation in Wyoming is probably the Eocene volcanic field in the Yellowstone-Absaroka region to the north of the Green River depositional basin (Love, 1939; Hay, 1956; Ebens, 1963).

AUTHIGENIC MINERALOGY

The vitric matrix of the tuff generally is altered to clinoptilolite, heulandite, a phase intermediate between clinoptilolite and heulandite, mordenite, analcime, potassium feldspar, quartz, and clay minerals. Pyrite,

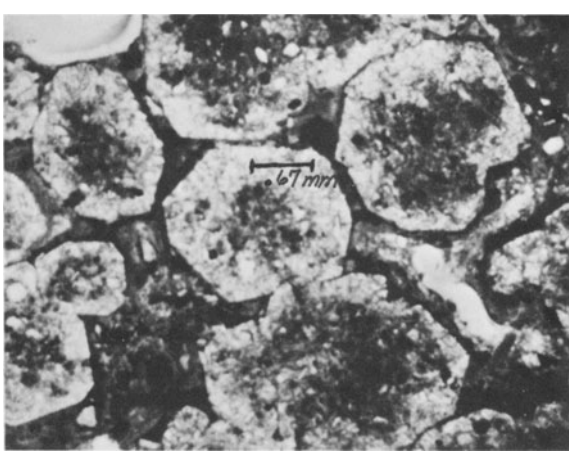

Figure 6. Photomicrograph of the trapezohedrons of analcime in the analcime-rich facies. Dark outlines around the crystals are hematite. The crystals are mottled by inclusions of pyroclastic grains.

https://doi.org/10.1346/CCMN.1981.0290506 Published online by Cambridge University Press

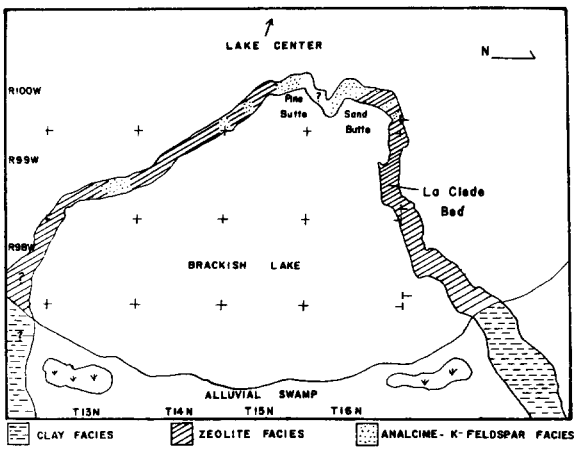

Figure 7. Authigenic mineral facies in the tuff (ZT). The paleogeographic interpretation is from Surdam and Stanley (1978).

chert, and minor amounts of such weathering products as gypsum, anhydrite, and iron oxides are also present in many samples.

Distribution of the authigenic minerals

Goodwin (1971) and Surdam and Parker (1972) recognized four major authigenic silicate mineral zones (or facies) in the tuffs of the Green River Formation, each representing a successive stage in a sequence of alteration. These zones are: (1) clay minerals, (2) alkali-rich zeolite, (3) analcime, and (4) K-feldspar. The tuff in this study incorporates elements of all four zones, but only the zeolite and analcime zones were sampled in detail.

Roehler (1972) described a montmorillonite-rich mineral facies in strata of the same interval as the tuff in a region outside the area of investigation (landward of the inferred ancient shoreline in a basin-margin facies). In the area of investigation, however, the tuff has altered to zeolites with sporadic occurrences of analcime associated with potassium feldspar. The non-analcime zeolite facies contains mordenite, clinoptilolite, heulandite, and an intermediate heulandite-clinoptilolite. The analcime-K-feldspar facies is present in irregular and discontinuous patches. Figure 7 shows the distribution of the mineral zones.

Heulandite-group zeolites

Clinoptilolite was recognized in the Tipton Shale Member of the Green River Formation by Goodwin and Surdam (1967), and Surdam and Parker (1972) and Roehler (1972) identified it in some of the tuffaceous sediments of the Laney Member. However, true heulandite or other members of the heulandite group have not been previously recognized in the Green River Formation.

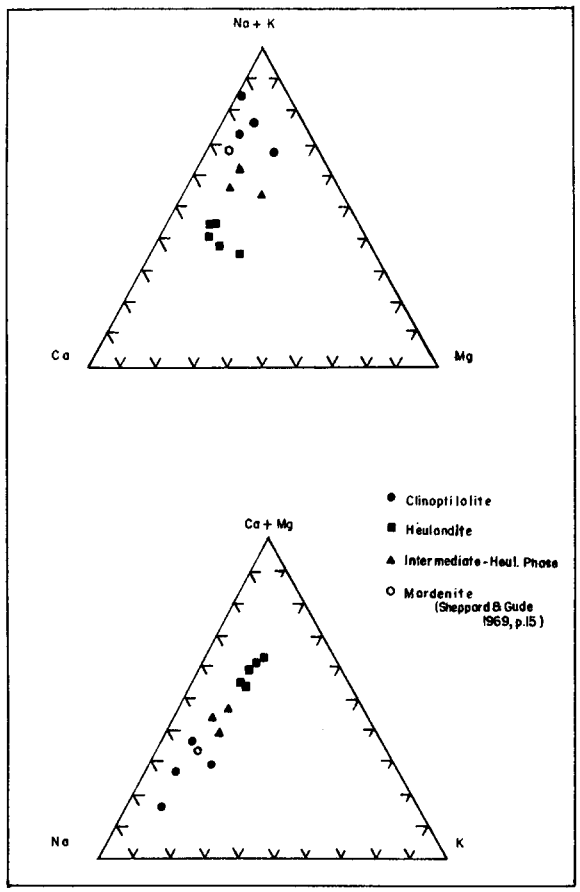

Figure 8. Ternary diagram showing the correlation between the heulandite-group zeolites and exchangeable cations. Analyses are from Tables 2–4, plus samples 3-74 and S3-71.

The heulandite-group zeolites were studied using the heat-treatment techniques of Mumpton (1960) and Boles (1972). Some samples, after heating at 500°C for 12 hr, retain 10–50% of the basal peak intensity. These samples fit neither the criteria for heulandite (>90% intensity loss) nor clinoptilolite (<50% intensity loss) and are considered to be an intermediate phase between these two end members. The intermediate thermal properties may be explained by: (1) zoned crystals (Shepard, 1961); (2) a mixture of clinoptilolite and heulandite; or (3) a chemically homogeneous, alkali-rich heulandite, perhaps the result of cation exchange after crystallization (Shepard and Starkey, 1964).

The Ca content (Table 2) of heulandites is higher than the Na and K contents; whereas, in the clinoptilolites the alkalies exceed Ca, and Na is dominant over K. Si/(Al + Fe^{3+}) ratios range from 4.2 to 5.1, and no significant differences were found between ratios in the different heulandite-group zeolites. From these data, the heulandite-group zeolites examined here appear to be best distinguished on the basis of cation content (Figure 8).

https://doi.org/10.1346/CCMN.1981.0290506 Published online by Cambridge University Press

Clinoptilolite and heulandite occur as clear laths or coffin-shaped plates having low birefringence, and they form the very fine to fine-grained felted matrix of the tuff. The crystals are about 1–100 μm in length, however, most are less than 2 μm long (Figure 9). The larger crystals form pseudomorphs of shards and have grown perpendicular to shard walls and fill interstitial cavities. Clinoptilolite, heulandite, and the intermediate phases are absent where the tuff is analcime rich, but are present from trace amounts to nearly 100% in all other samples of the tuff (Table 1). The minerals are generally associated with one or more of the following other authigenic minerals: mordenite, analcime, potassium feldspar, clay minerals, quartz.

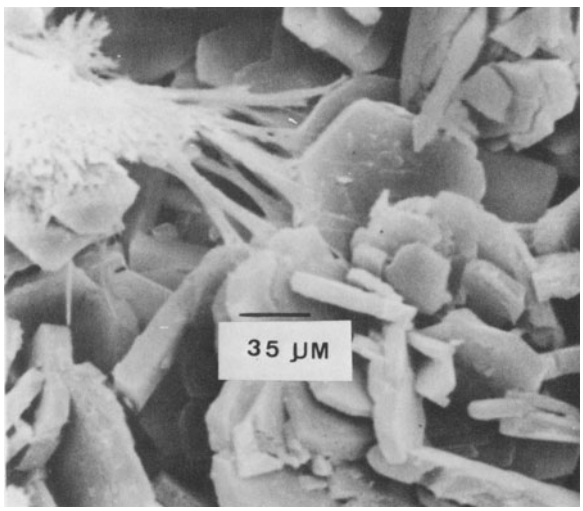

Figure 9. Scanning electron micrograph showing the textural relationship between lath-shaped clinoptilolite and fibrous mordenite.

Mordenite

Mordenite was first recognized in the Tipton Member of the Green River Formation by Goodwin and Surdam (1967) and in the Laney Member by Surdam and Parker (1972). In the present study, mordenite was identified by XRD data and by crystal morphology using SEM. Mordenite is characteristically fibrous and forms bundles or delicate webs in close association with heulandite or clinoptilolite (Figure 9). Mordenite is typically a very siliceous zeolite with a Si/(Al + Fe^{3+}) ratio of 4.5 to 5.3; Na and Ca are generally the dominant exchangeable cations, but K and Mg are commonly present (Sheppard and Gude, 1973). Mordenite makes up less than 20% of any sample of the tuff examined. Attempts to separate mordenite from the more abundant heulandite-group zeolites were unsuccessful; therefore, no chemical analyses were made. A published analysis, however, of relatively pure mordenite from another sedimentary locality (Sheppard and Gude, 1969, p. 15) is given in Table 2 and is plotted in Figure 8.

Analcime

Analcime was noted in amounts varying from trace to >90% in three modes of occurrence: (1) as a microcrystalline component in tuffs rich in heulandite, clinoptilolite, or mordenite; (2) as concentrations in thin laminations in the carbonate strata underlying and overlying the tuff (in thin section such analcime is isotropic, clear, and colorless or brownish, and forms nearly pure laminae); and (3) as coarse-grained crystals replacing the tuff bed (Figure 6).

Analcime is a sodium zeolite having Si/Al ratios of 1.5–2.9, with the more siliceous phases being found in altered rhyolitic tuffs (Coombs and Whetten, 1967; Iijima and Hay, 1968). The compositions of the analcimes analyzed in this study were determined by three methods: (1) chemical analyses of analcime separates (Table 3), (2) X-ray energy spectrometry (XES) of individual grains during SEM, and (3) Saha's XRD method (1959, 1961) using the calibration curve of Coombs and Whetten (1967). The Si/Al ratios obtained by chemical analyses and XES methods are given in Table 4. Saha's method utilizes unit-cell size as an indicator of composition. The broad XRD 639 reflections given by the

Table 4. Comparative Si:Al ratios of analcimes.

Sample	Wet chemical analyses[1]				XES[2]	
	Si:Al	Si/unit cell	Si:(Al + Fe^{3+})	Si/unit cell	Si:Al	Si/unit cell
18-T1	3.01	36.03	2.89	35.65	3.2	36
S1-T2	3.06	36.18	2.86	35.56	3.1	36
22-TA	3.06	36.18	2.88	35.64	2.7	35
S6-T	3.08	36.23	2.81	35.40	2.9	36
S1-T10A	3.06	36.18	2.86	35.56	3.0	36
10-T2	3.02	36.06	2.97	35.91	3.0	36

[1] Complete analyses are listed in Table 3.
[2] Average ratio of counts.

https://doi.org/10.1346/CCMN.1981.0290506 Published online by Cambridge University Press

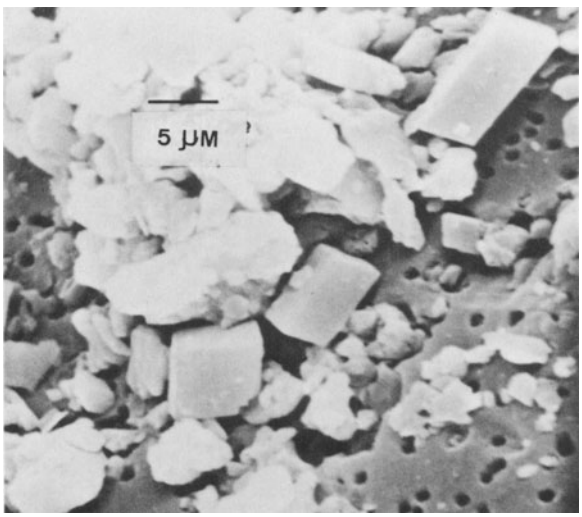

Figure 10. Scanning electron micrograph showing euhedra of authigenic K-feldspar and quartz growing on a pitted analcime.

analcime in this study indicate variable compositions of the crystals within a single sample; therefore, the XRD data give only general compositions. Nevertheless the XRD method indicates lower Si/Al ratios than the other methods, an enigma also encountered by Goodwin (1971) in his study of analcimes in the Green River tuffs. Minute silica inclusions in the analcime may be responsible for differences in Si/Al ratio.

Potassium feldspar

K-feldspar in the tuff bed is associated with authigenic quartz and pitted analcime crystals (Figure 10). It occurs in trace quantities as individual monoclinic crystals, generally <4 μm in length. It was not recognized in thin section as overgrowths or replacements of other grains, and therefore is considered authigenic. Analyses by XES indicate that the crystals are a pure potassium variety. In sample 17-T, the K-feldspar is associated with a heulandite-group zeolite.

Authigenic K-feldspar in the Wilkins Peak and Laney Members was described by Hay (1966), Iijima and Hay (1968), Goodwin (1971), and Surdam and Parker (1972) and makes up as much as 95% of many of the tuff beds in those stratigraphic intervals. Based on XRD data, the K-feldspar in this study appears identical to the monoclinic variety found in the above studies and in other similar sedimentary environments (Hay and Moiola, 1963; Sheppard and Gude, 1968, 1969).

Quartz

Detrital quartz is present in all samples. Authigenic quartz was identified only in the analcime-rich parts of the tuff associated with K-feldspar. A few pyroclastic grains of quartz are replaced by chert.

Biotite and clay minerals

Except in trace quantities in the matrices of some tuff samples, clay minerals were not detected in the strata studied. Biotite of pyrogenic origin is present in most tuff samples.

Carbonate minerals

Calcite and dolomite were not detected in the tuff bed but make up as much as 75% of the carbonate strata above and below the tuff. Chemical analyses of the carbonates show that dolomite constitutes less than 10% of any sample, even if all magnesium in the sample is attributed to dolomite.

Other minerals

Pyrite or remnants of pyrite octahedra are found locally in most tuff and carbonate samples. Pyrite also occurs as cubes up to 0.2 mm in size, but it is commonly less than 0.05 mm. Iron oxides stain the outcrop and are found as alteration products of pyrite octahedra. Iron oxides also occur as cement outlining coarse analcime crystals.

Calcite and gypsum rarely replace other minerals. Gypsum occurs as a late weathering product in the carbonate strata above and below the tuff. Anhydrite is associated with, or replaces, gypsum in most of these samples.

Paragenesis of the authigenic silicates

Most of the paragenetic relations observed in this study are well documented in studies by Iijima and Hay (1968), Sheppard and Gude (1969, 1973), Hay (1970), and Boles (1972). All samples showing shard textures contain alkalic zeolites as the major authigenic mineral. No sample located near the zone of unaltered glass contains analcime. SEM scans show that heulandite formed from and around the relict glass (Figure 11). In contrast to Sheppard and Gude's (1969) proposal that relict shard structures or vitroclastic textures are preserved by early clay rims, the shards encountered in this study that had been replaced by heulandite, clinoptilolite, or intermediate heulandite-clinoptilolite minerals show little evidence of clay rims. The glass → clinoptilolite reaction was documented by Sheppard and Gude (1969, 1973), Hay (1970), and Boles (1972).

No evidence was found suggesting that one alkalic zeolite replaced another. No discernable pattern of distribution of the alkalic zeolites was noted, and the differences in the nature of the exchangeable cations of the alkalic zeolites in the tuff must be due to local alkali activity differences or post-crystallization cation exchange.

In the field, the coarse-grained analcime nodules appear to replace fine-grained tuff. Complete loss of vitroclastic texture is common in the analcime facies. Where analcime occurs in the fine-grained matrix, it

https://doi.org/10.1346/CCMN.1981.0290506 Published online by Cambridge University Press

must have replaced the earlier formed heulandite-group zeolites, although this reaction can not be proven. Sheppard and Gude (1969), however, documented this reaction by identifying clinoptilolite-pseudomorphed shards partly replaced by analcime. Also, analcime that formed from heulandite-group zeolites (including clinoptilolite) has been shown to have a high silica content, greater than 34.5 Si atoms per unit cell (Sheppard and Gude, 1969). Analcime in the present study has a Si content of 35.0 to 36.2 atoms per unit cell (Table 3) supporting the above reaction.

SEM scans show authigenic K-feldspar and quartz on pitted and etched surfaces of partially dissolved analcime crystals (Figure 10), suggesting that the K-feldspar and quartz formed during and/or after the analcime began to dissolve. The reaction of analcime to K-feldspar is well documented by Iijima and Hay (1968).

Pyroclastic plagioclase grains are etched and pitted and are associated with minor amounts of clay minerals. The clay minerals are dirty-gray, irregular patches in the clear zeolitic matrixes and are probably products of late reactions with ground water.

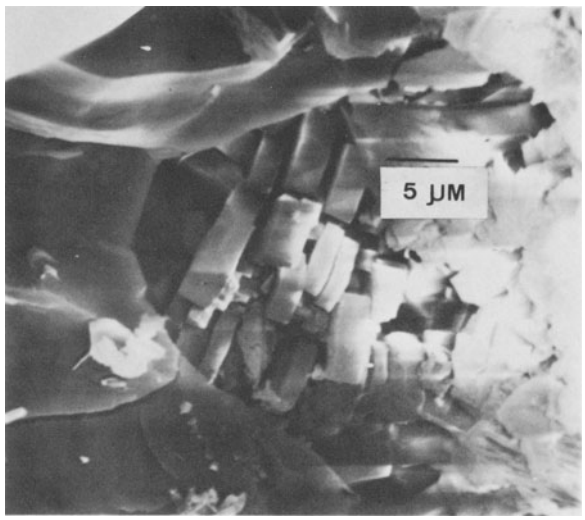

Figure 11. Scanning electron micrograph showing heulandite laths (edge view) adjacent to a glass shard.

GENESIS OF THE AUTHIGENIC MINERALS AND WATER CHEMISTRY

Controlling parameters

Hay (1966) suggested that three major factors control the formation and distribution of zeolites and other authigenic silicate minerals: (1) initial composition and age of the host rock; (2) variation in temperature and pressure; and (3) chemistry of the pore waters. The host rock of the present study is a highly siliceous vitric ash which formed as the result of a single volcanic episode. The ash bed probably had a similar original composition and texture throughout the study area. Shallow burial of the Laney Member indicates that temperatures have not exceeded 100°C and pressures have not exceeded 400 bars (Goodwin, 1971). Therefore, the occurrence and distribution of the authigenic silicates in the tuff and carbonate strata reflect the chemistry of the interstitial pore fluids present during diagenesis. Several factors are influential in determining whether clay minerals, zeolites, or feldspars will form when pore solutions react with vitric material in the host rocks. These factors, which also control the paragenetic relations among the authigenic minerals, are: (1) salinity, (2) a_{H_2O}, (3) a_{SiO_2}, (4) pH, and (5) relative proportions of the alkali and alkaline earth cations, i.e., Na^+, K^+, Ca^{2+}, and Mg^{2+} (Hay, 1966; Sheppard and Gude, 1968; Surdam and Mariner, 1972).

Lake Gosiute was a saline, alkaline lake in a hydrographically closed basin until late Laney time (Surdam and Stanley, 1979). This lake provided an ideal setting for the hydration and solution of volcanic glass and for the subsequent precipitation of zeolites (Surdam and Sheppard, 1978). Figure 7 shows the distribution of clay minerals, zeolites, and analcime in the stratigraphic interval studied.

Clay mineral reactions

The clay mineral facies which lies outside the area of investigation, is montmorillonite-rich and contains no zeolites (Roehler, 1972). These rocks were deposited at the basin margin in an alluvial environment and were in contact with only dilute surface runoff. Because the rocks never came in contact with the saline waters of the lake, fluids in contact with these rocks did not have high enough salinities and alkalinities to produce zeolites.

Reactions forming zeolites

The topographic gradient of the lake bottom was about 18 cm/km (1 ft/mile), so that relatively small changes in the depths of the lake caused large changes in the shoreline. Surdam and Stanley (1979) showed that during the time the tuff was deposited, the lake shore could have fluctuated from the position shown on Figure 7 (maximum stand) to a position in the vicinity of Pine Butte and Sand Butte (minimum stand). These fluctuations were a function of the imbalance between inflow and evaporation related to seasonal and climatic variations. The potential for significant variations in lake and interstitial waters associated with the tuff bed was great. In addition, the area between the high and low stands of the lake (fringing mudflat) was dotted by springs as recorded in the sediments by tufa deposits. The tufa deposits are associated with the zeolitic tuff. These springs locally would have had a significant effect on the composition of the pore fluids. Variations in the fluids caused by general fluctuations in the lake

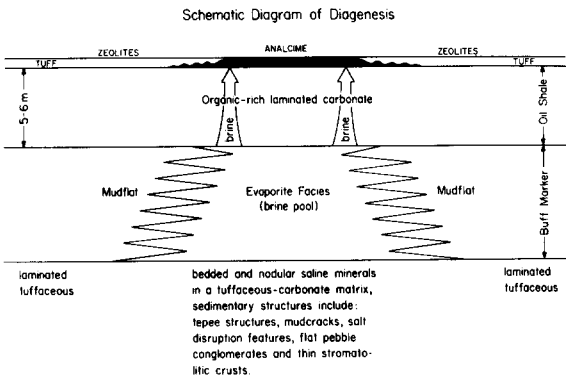

Figure 12. Schematic diagram of the diagenetic process resulting in the zeolite → analcime reaction in the tuff bed.

chemistry and locally by the influence of springs probably were significant enough to cause the observed variations in alkalic zeolite chemistry.

It is also possible that the early dolomitization of calcite in both the underlying and overlying carbonate strata provided Ca^{2+} to the fluids in the adjacent tuff. If this diagenetic process did not determine the zeolite mineralogy (i.e., heulandite or clinoptilolite), it probably initiated some cation exchange in the zeolites.

Reactions forming analcime

The reaction of alkalic zeolites to analcime is common in saline, alkaline-lake deposits (Surdam and Sheppard, 1978) and is favored by high activities of Na^+ and by low activities of silica. The analcime-rich parts of the tuff are closely related to brine-pool deposits in the underlying Buff Marker (Figure 12). Trona and nahcolite were deposited in these brine pools. During subsequent diagenesis, these brine-pool deposits were a source of Na-rich waters. The alkalic zeolite → analcime reaction apparently started at the base of the tuff and proceeded upward (Figure 5). Commonly, the analcime nodules in the zeolite-rich tuff are spatially related to fractures (fluid pathways) in the underlying oil shale (Figure 5). The brine-pool deposits were possibly the source of Na-enriched fluids that reacted with alkalic zeolites to form analcime. In contrast, where the zeolitic tuff overlies mudflat deposits, the water released during diagenesis would be similar in composition to the interstitial fluid already in the tuff; hence the only reaction may have been some cation exchange.

Minor amounts of K-feldspar may have formed at the expense of analcime (Figure 10). This reaction is probably a function of Na/K ratio of the interstitial fluids; where the activity of K^+ was elevated, authigenic K-feldspar formed.

CONCLUSIONS

The diagenesis of a thin tuff bed in the Laney Member of the Green River Formation was characterized principally by hydration and solution of volcanic glass by saline, alkaline fluids and by the precipitation of zeolites. These early reactions involved only minor mass transfer on a very small scale, exclusive of H_2O and probably proceeded from the time of deposition of the ash bed through early diagenesis. Variations in the early zeolite mineralogy were a function of differences in the composition of the interstitial fluid caused by either fluctuations in lake-water chemistry or by the proximity of spring discharge.

Dehydration and Na-metasomatism occurred later in the diagenetic history of the tuff bed and involved dehydration and addition of Na to the early-formed zeolites to form analcime. The dehydration reactions proceeded after burial and involved significant mass transfer.

ACKNOWLEDGMENTS

We thank S. Boese, J. I. Drever, J. Murphy, and K. O. Stanley for many helpful discussions. This work was supported in part by a grant from the Marathon Oil Company.

REFERENCES

Boles, J. R. (1972) Composition, optical properties, cell dimensions, and thermal stability of some heulandite group minerals: *Amer. Mineral.* **57,** 1463–1493.

Bradley, W. H. (1964) Geology of the Green River Formation and associated Eocene rocks in southwestern Wyoming and adjacent parts of Colorado and Utah: *U.S. Geol. Surv. Prof. Pap.* **496-A,** 86 pp.

Bradley, W. H. and Eugster, H. P. (1969) Geochemistry and paleolimnology of the trona deposits and associated authigenic minerals of the Green River Formation of Wyoming: *U.S. Geol. Surv. Prof. Pap.* **496-B,** 71 pp.

Breck, D. W. (1974) *Zeolite Molecular Sieves: Structure, Chemistry, and Use:* Wiley, New York, 771 pp.

Buchheim, H. P. (1978) Paleolimnology of the Laney Member of the Eocene Green River Formation: Ph.D. thesis, Univ. Wyoming, Laramie, Wyoming, 101 pp. (unpublished).

Coombs, D. S. and Whetten, J. T. (1967) Composition of analcime from sedimentary and burial metamorphic rocks: *Geol. Soc. Amer. Bull.* **78,** 269–282.

Ebens, R. J. (1963) Petrography of the Eocene Tower Sandstone lenses at Green River, Sweetwater County, Wyoming: M.S. thesis, Univ. Wyoming, Laramie, Wyoming, 46 pp. (unpublished).

Goodwin, J. H. (1971) Authigenesis of silicate minerals in tuffs of the Green River Formation, Wyoming: Ph.D. thesis, Univ. Wyoming, Laramie, Wyoming, 98 pp.

Goodwin, J. H. and Surdam, R. C. (1967) Zeolitization of tuffaceous rocks of the Green River Formation, Wyoming: *Science* **157,** 307–308.

Hay, R. L. (1956) Pitchfork Formation, detrital facies of early basic breccia, Absoraka Range, Wyoming: *Amer. Assoc. Pet. Geol. Bull.* **40,** 1863–1898.

Hay, R. L. (1966) Zeolites and zeolitic reactions in sedimentary rocks: *Geol. Soc. Amer. Spec. Pap.* **85,** 130 pp.

Hay, R. L. (1970) Silicate reactions in three lithofacies of a semi-arid basin Oldavai Gorge, Tanzania: *Mineral. Soc. Amer. Spec. Pap.* **3,** 237–255.

Hay, R. L. and Moiola, R. J. (1963) Authigenic silicate min-

erals in Searles Lake, California: *Sedimentology* **2,** 312–332.
Iijima, Azuma and Hay, R. L. (1968) Analcime composition in tuffs of the Green River Formation of Wyoming: *Amer. Mineral.* **53,** 184–200.
Love, J. D. (1939) Geology along the southern margin of the Absaroka Range, Wyoming: *Geol. Soc. Amer. Spec. Pap.* **20,** 134 pp.
Mumpton, F. A. (1960) Clinoptilolite redefined: *Amer. Mineral.* **45,** 351–369.
Roehler, H. W. (1969) Stratigraphy and oil shale deposits of Eocene rocks in the Washakie Basin, Wyoming: in *Tertiary Rocks of Wyoming,* Wyoming Geol. Assoc. Guidebook 21st Field Conference, 197–206.
Roehler, H. W. (1972) Zonal distribution of montmorillonite and zeolites in the Laney Shale Member of the Green River Formation in the Washakie Basin: *U.S. Geol. Surv. Prof. Pap.* **800-B,** B123–126.
Roehler, H. W. (1973) Stratigraphic divisions and geologic history of the Laney Member of the Green River Formation in the Washakie Basin in southwestern Wyoming: *U.S. Geol. Surv. Bull.* **1372-E,** E1–E28.
Saha, Presejit (1959) Geochemical and X-ray investigations of natural and synthetic analcites: *Amer. Mineral.* **44,** 300–313.
Saha, Presejit (1961) The system $NaAlSiO_4$ (nepheline)–$NaAlSi_3O_8$ (albite)–H_2O: *Amer. Mineral.* **46,** 859–884.
Shepard, A. O. (1961) A heulandite-like mineral associated with clinoptilolite in tuffs of Oak Spring Formation, Nevada Test Site, Nye County, Nevada: *U.S. Geol. Surv. Prof. Pap.* **424-C,** C320–323.
Shepard, A. O. and Starkey, H. C. (1964) Effect of cation exchange on the thermal behavior of heulandite and clinoptilolite: *U.S. Geol. Surv. Prof. Pap.* **475-D,** 89–92.
Sheppard, R. A. and Gude, A. J., 3rd (1968) Distribution and genesis of authigenic silicate minerals in tuffs of Pleistocene Lake Tecopa, Inyo County, California: *U.S. Geol. Surv. Prof. Pap.* **597,** 38 pp.
Sheppard, R. A. and Gude, A. J., 3rd (1969) Diagenesis of tuffs in the Barstow Formation, Mud Hills, San Bernardino County, California: *U.S. Geol. Surv. Prof. Pap.* **634,** 35 pp.
Sheppard, R. A. and Gude, A. J., 3rd (1973) Zeolites and associated authigenic silicate minerals in tuffaceous rocks of the Big Sandy Formation, Mohave County, Arizona: *U.S. Geol. Surv. Prof. Pap.* **830,** 36 pp.
Surdam, R. C. and Eugster, H. P. (1976) Mineral reactions in the sedimentary deposits of the Lake Magadi region, Kenya: *Geol. Soc. Amer. Bull.* **87,** 1739–1752.
Surdam, R. C. and Parker, R. B. (1972) Authigenic aluminosilicate minerals in the tuffaceous rocks of the Green River Formation, Wyoming: *Geol. Soc. Amer. Bull.* **83,** 689–700.
Surdam, R. C. and Sheppard, R. A. (1978) Zeolites in saline, alkaline-lake deposits: in *Natural Zeolites: Occurrence, Properties, Use,* L. B. Sand and F. A. Mumpton, eds., Pergamon Press, Elmsford, New York, 145–174.
Surdam, R. C. and Stanley, K. O. (1979) Lacustrine sedimentation during the culminating phase of Eocene Lake Gosiute, Wyoming (Green River Formation): *Geol. Soc. Amer. Bull. Pt. 1,* **90,** 93–110.
Surdam, R. C. and Mariner, R. (1972) The genesis of phillipsite in Recent tuffs at Teels Marsh, Nevada: Program, 1971 Annual Meet. Geol. Soc. Amer., p. 725. (abstract).

(Received 11 December 1980; accepted 24 June 1981)

Резюме—Две диагенетические стадий цеолитовой перемены были найдены при исследовании тонкого слоя риолитового попела, который был осажден в эоценовом озере Госют (член Ляней формации Зеленой Реки). Слой попела может прослеживаться на расстоянии 30 км вдоль местонахождения и является представителем одного вулканического события. Этот слой не был погребен глубоко (<100°C) и первоначально был гомогеническим по составу. Сначала слой изменился в клиноптилолит, голандит, промежуточную фазу между этими двумя цеолитами, и морденит. Ранние реакции включали в себя пидратацию и растворение стекла соляновыми, щелочными растворами, а также последующее осаждение цеолитов. Изменение минералогии цеолитов происходило благодаря разницам в химии трещинных жидкостей, что было результатом флуктуации химии озерных вод или близкости весенних опадов. Эти реакции, исключая добавление H_2O, включали только незначительные количества переноса массы на очень малые расстояния. Позднее, после погребения, первоначально образованные цеолиты реагировали с всходящими потоками соляновых растворов карбонатов натрия, которые были продуктом отводнения расподоженных ниже осадков эвапорита. Соляновые растворы карбонатов натрия в равновесии с троной и нахколитом увеличили активность Na^+ и образовали анальцим. Эти поздние реакции дегидратации включали значительный перенос массы. [E.C.]

Resümee—Bei einer Untersuchung einer dünnen rhyolithischen Aschenlage, die im eozänen Lake Gosiute (Laney Schicht der Green River Formation) abgelagert wurde, wurden zwei diagenetische Stadien der Zeolithumwandlung beobachtet. Die Aschenlage kann über eine Strecke von 30 km verfolgt werden und stellt ein einziges vulkanisches Ereignis dar. Die Lage wurde nicht sehr überlagert (<100°C) und hatte ursprünglich eine homogene Zusammensetzung. Zu Beginn wurde die Lage in Klinoptilolith, Heulandit und in ein Zwischenglied dieser beiden Zeolithe sowie in Mordenit umgewandelt. Diese frühen Reaktionen beinhalteten die Hydratation und Auflösung des Glases durch saline alkalische Lösungen und die darauf folgende Ausfällung der Zeolithe. Die Variation der Zeolithe hängt mit dem unterschiedlichen Chemismus der Porenlösung zusammen, der entweder durch Schwankungen im Chemismus des Seewassers hervorgerufen wurde oder durch die Nähe von Quellen. Diese Reaktionen bedeuten, mit Ausnahme der H_2O-Zufuhr, nur einen geringen Stofftransport über sehr kleine Entfernungen. Später, nach der Überdeckung, reagierten die früher gebildeten Zeolithe mit aufsteigenden Natriumkarbonat-Lösungen, die durch die Entwässerung der darunterliegenden Evaporitablagerungen entstanden sind. Die Natriumkarbonat-Lösungen, die im Gleichgewicht mit Trona und Nahcolith sind, erhöhten die Na^+-Aktivität, und führten zur Bildung von Analcim. Diese späteren Dehydratationsreaktionen beinhalten einen erheblichen Stofftransport. [U.W.]

Résumé—Deux étapes diagénétiques d'altération zéolitique ont été reconnues au cours de l'étude d'un mince lit de cendres rhyolitiques déposé dans le Lac Gosiute éocène (Membre Laney de la Formation Green River). La couche de cendres peut être tracée pendant 30 km suivant sa direction et représente un seul évènement volcanique. La couche n'est pas ensevelie profondément (<100°C), et était à l'origine de composition homogène. Initialement, la couche s'était altérée en clinoptilolite, heulandite, une phase intermédiaire entre ces deux zéolites, et en mordénite. Ces réactions précoces impliquaient l'hydration et la solution du verre par des solutions salines, alkalines, et la précipitation ultérieure de zéolites. La variation minéralogique de la zéolite est due à des différences dans la chimie du fluide interstitial résultant soit de fluctuations de la chimie de l'eau du lac, soit de la proximité de la décharge d'une source. Ces réactions, excluant l'addition d'H_2O, n'impliquaient que de petites quantités de transfert en masse sur de très petites distances. Plus tard, après l'enterrement, les zéolites formées précocément ont réagi avec des saumures de carbonate de sodium ascendantes, qui avaient été produites par la perte d'eau de dépôts d'évaporites sousjacents. Les saumures de carbonate de sodium, en équilibre avec trona et nahcolite, ont élevé l'activité de Na^+ et ont produit l'analcime. Ces réactions de déshydration tardives impliquaient un transfert en masse significatif. [D.J.]

https://doi.org/10.1346/CCMN.1981.0290506 Published online by Cambridge University Press